

1 **Nasal cavity of green sea turtles contains three independent sensory epithelia**

2

3 Daisuke Kondoh^{1*}, Chiyo Kitayama², Yohei Yamaguchi¹, Masashi Yanagawa³,
4 Yusuke K. Kawai⁴, Chihiro Suzuki¹, Raito Itakura¹, Atsuru Fujimoto⁵, Tadatoshi Satow⁵,
5 Satomi Kondo², Takayuki Sato²

6

7 ¹Laboratory of Veterinary Anatomy, Obihiro University of Agriculture and Veterinary
8 Medicine, Obihiro, Hokkaido 080-8555, Japan

9 ²Everlasting Nature of Asia (ELNA), Ogasawara Marine Center, Ogasawara, Tokyo 100-
10 2101, Japan

11 ³Department of Applied Veterinary Medicine, Obihiro University of Agriculture and
12 Veterinary Medicine, Obihiro, Hokkaido 080–8555, Japan

13 ⁴Laboratory of Toxicology, Obihiro University of Agriculture and Veterinary Medicine,
14 Obihiro, Hokkaido 080–8555, Japan

15 ⁵Division of Environmental and Agricultural Engineering, Obihiro University of
16 Agriculture and Veterinary Medicine, Obihiro, Hokkaido 080-8555, Japan

17

18 Correspondence to be sent to: Daisuke Kondoh, Laboratory of Veterinary Anatomy,
19 Obihiro University of Agriculture and Veterinary Medicine, Obihiro, Hokkaido 080-8555,
20 Japan. email: kondoh-d@obihiro.ac.jp

21

22 **Keywords:** computed tomography; histology; odorant receptor; olfactory system; reptile;
23 vomeronasal organ.

24

25 **Abstract**

26 The morphological and histological features of the nasal cavity are diverse among
27 animal species, and the nasal cavities of terrestrial and semi-aquatic turtles possess two
28 regions lined with each different types of sensory epithelium. Sea turtles can inhale both
29 of volatile and water-soluble odorants with high sensitivity, but details of the architectural
30 features and the distribution of the sensory epithelia within the sea turtle nasal cavity
31 remain uncertain. The present study analyzed the nasal cavity of green sea turtles using
32 morphological, computed tomographic and histological methods. We found that the
33 middle region of the sea turtle nasal cavity is divided into anterodorsal, anteroventral and
34 posterodorsal diverticula and a posteroventral excavation by connective tissue containing
35 cartilages. The posterodorsal diverticulum was lined with a thin sensory epithelium, and
36 the anterodorsal and anteroventral diverticula were occupied by a single thick sensory
37 epithelium. In addition, a relatively small area on the posteroventral excavation was
38 covered by independent sensory epithelium that differed from other two types of epithelia,
39 and a single thin bundle derived from the posteroventral excavation comprised the most
40 medial nerve that joins the anterior end of the olfactory nerve tract. These findings
41 suggested that the posteroventral excavation identified herein transfers stimuli through an
42 independent circuit and plays different roles when odorants arise from other nasal regions.

43 (214 words)

44

45 **Introduction**

46 Nasal morphological features are diverse among animal species, and the nasal
47 cavity in vertebrates contains sensory epithelia that function as an olfactory organ.
48 Sensory epithelia associated with olfactory system in most tetrapods are generally divided
49 into the olfactory and vomeronasal epithelia that project to the main and accessory
50 olfactory bulbs, respectively (Taniguchi and Taniguchi 2014). Both types of epithelia are
51 histologically pseudostratified and generally comprises the supporting, receptor and basal
52 cells. Nuclei of the supporting cells are generally oval and form a zone at the top region
53 of the epithelium. Nuclei of the receptor cells form the zone of round nuclei in the middle
54 of the epithelium. Basal cells are progenitors of receptor and supporting cells and are
55 located at the bottom of the epithelia (Gunasegaran 2010).

56 In terms of phylogenetical theory, most fishes possess only a single type of sensory
57 epithelium associated with olfaction, whereas amphibians have a vomeronasal epithelium
58 that covers the ventral region of the nasal cavity, and squamates and most mammals have
59 a vomeronasal organ that is completely separate from the nasal cavity (Romer and Parsons
60 1977; Kondoh et al. 2010; Taniguchi and Taniguchi 2014). In contrast, crocodiles and
61 birds have lost this organ and have only olfactory epithelium in the nasal cavity (Romer
62 and Parsons 1977; Kondoh et al. 2011). Turtles do not have a separate vomeronasal organ,
63 but they have two regions in the nasal cavity lined with different types of sensory epithelia
64 (Graziadei and Tucker 1969; Nakamuta N et al. 2016; Nakamuta S et al. 2016). However,
65 whether any of these types of epithelia corresponds to vomeronasal epithelium remains
66 debatable.

67 Turtles split from the bird-crocodilian lineage approximately 250 million years ago
68 (Wang et al. 2013). The oldest fossil of a candidate sea turtle, *Odontochelys*, is from the

69 Triassic period about 220 million years ago (Li et al. 2008), but sea turtles existed during
70 the Lower Cretaceous period about 108 million years ago (Hirayama 1998). Sea turtles
71 belong to the suborder Testudines, the order Cryptodira, superfamily Chelonioidea, and
72 are presently classified into seven species (two families and six genera). Green sea turtles
73 (*Chelonia mydas*) reach sexual maturity after 20 - 50 years (Balazs 1982; Frazer and
74 Ehrhart 1985) and lay eggs on beaches. These eggs hatch after two months, and the
75 hatchlings move to the horizon according to “low horizon elevation” (Limpus and
76 Kamrowski 2013), although the ecology of sea turtles during this period remains largely
77 unknown. Small juveniles are polyphagous and spend time offshore, whereas developed
78 turtles (straight carapace length: > 0.3 m) populate coastal areas and become mainly
79 herbivorous. Sea turtles make developmental and seasonal migrations. Green sea turtles
80 return to the beach where they were born (homing behavior) to breed (Bowen and Karl
81 2007), but how and when they imprint the home beach remains unknown.

82 Sea turtles intake both volatile and water-soluble odorants with high sensitivity
83 (Manton et al. 1972; Endres et al. 2009; Endres and Lohmann 2013), although their
84 lifestyle is uniquely marine. The structure of the sea turtle nasal cavity is more complex
85 than those of terrestrial or semi-aquatic turtles, and reports indicate that it has three
86 diverticula (Parsons 1968; Saito et al. 2000). However, details of the architectural features
87 and the distribution of the sensory epithelia within the sea turtle nasal cavity remain
88 uncertain because few individuals have been analyzed and non-destructive verification is
89 scant. Here, we analyzed the nasal cavity of juvenile green sea turtles in detail using
90 morphological and histological methods as well as computer tomographic (CT) imaging.

91

92 **Materials and methods**

93 **Animals**

94 We analyzed seven juvenile turtles (age, < 6 months) of unknown sex that were
95 hatched, bred and died naturally at Ogasawara Marine Center (Japan), and a juvenile turtle
96 that became stranded on the coast of Chichi-Jima in the Ogasawara Islands, Japan. The
97 heads of the former seven turtles were rapidly fixed and preserved in natural formalin.
98 The head of the stranded turtle was stored frozen for CT imaging. This study proceeded
99 in accordance with the guidelines for the Regulations on the Management and Operation
100 of Animal Experiments, and the Animal Care and Use Committee of Obihiro University
101 of Agriculture and Veterinary Medicine approved the experimental protocol (Notification
102 number 28-44).

103

104 **Morphological procedures**

105 The nasal regions of four turtles were assessed in the left-lateral view after
106 removing the encircling maxillary and prefrontal bones. The lateral half of the left nasal
107 regions was then removed to evaluate the internal structures of the nasal cavity. The
108 remaining medial half of the left nasal regions of three specimens were removed, and then
109 the distribution of nerves derived from the right nasal cavity to the olfactory bulb was
110 determined. The remaining specimen was cleared and double stained with Alcian blue
111 (pH 2.5) and alizarin red to visualize cartilages and bones, respectively.

112

113 **CT image analysis**

114 The frozen head of a turtle was assessed by CT using an Aquilion TSX-201A
115 scanner (Toshiba Medical Systems Corporation, Otawara, Japan) under the following

116 conditions: 120 kV, 250 mA and 0.5 mm slice thickness. Imaging data stored in DICOM
117 format were reconstructed into three-dimensional images using an AZE VirtualPlace
118 Fujin workstation (AZE Ltd., Tokyo, Japan). The internal architecture of the nasal cavity
119 was visualized using the software mode for outline detection of the lungs.

120

121 **Simulation of water inflow into the nasal cavity**

122 The DICOM files were processed using Fiji/ImageJ software (<http://fiji.sc/Fiji>).
123 The internal structure of the nasal region was extracted from sequenced 8-bit inverted
124 images on a threshold range of 200 to 255, reconstructed into three-dimensional images
125 with a 3D Viewer plugin (display as surface; threshold, 100; resampling factor, 2) and
126 imported as STL files, which were then trimmed using MeshLab software
127 (<http://meshlab.sourceforge.net>), smoothed (factor, 0.50; repeat, 1) and solidified
128 (thickness, 0.10) using Blender software (www.blender.org). These data were output at
129 three times the original size using 3DPrint Software (3D Systems Inc., Rock Hill, SC,
130 USA) and a ProJet 4500 printer (3D Systems). A transparent silicon mold (Zoukei-Mura
131 Inc., Kyoto, Japan) was made of the right side of the nasal cavity. One hole at each of the
132 anterior and posterior ends was drilled through the mold, which was gently submerged in
133 water at various angles.

134

135 **Histological procedures**

136 The nasal regions of three turtles were post-fixed in Bouin fixative overnight and
137 decalcified using Plank-Rychlo solution for four hours at room temperature. Samples
138 were embedded in paraffin using standard procedures and sliced into 5- μ m thick sections
139 at 20- μ m intervals. Some sections were deparaffinized, rehydrated and stained with

140 hematoxylin-eosin and others were processed for immunohistochemistry.

141

142 **Immunohistochemical procedures**

143 Receptor cells were immunohistochemically detected using the antibody A-21271
144 (Molecular Probes, Eugene, OR, USA) against HuC and HuD, which are RNA-binding
145 proteins that serve as markers of developing neurons in most vertebrate species, including
146 turtles (Nakamuta et al. 2018). Deparaffinized, rehydrated sections in Tris-EDTA buffer
147 (0.01 M, pH 9.0) were heated in a microwave oven for antigen retrieval. Thereafter, the
148 sections were incubated with 0.3% H₂O₂ in methanol for 30 min to eliminate endogenous
149 peroxidase, rinsed in phosphate-buffered saline (0.01 M, pH 7.4) three times and
150 incubated with 3% normal goat serum for one hour at room temperature to block
151 nonspecific binding. The sections were incubated with 1.0 µg/mL of A-21271 antibody
152 overnight at 4 °C, rinsed three times, and then incubated with 7.5 µg/mL of BA-9200
153 biotinylated secondary antibody (Vector Laboratories Inc., Burlingame, CA, USA) for
154 one hour at room temperature. After three rinses, the sections were reacted with PK-6100
155 avidin-biotin complex reagent (Vector) for 30 min, rinsed again, and then colored with
156 Tris-HCl buffer containing 0.02% 3,3'-diaminobenzidine tetrahydrochloride and 0.006%
157 H₂O₂ for 10 min at room temperature. The sections were mounted in MGK-S (Matsunami
158 Glass Industries, Osaka, Japan) and assessed using a Microphot-FX microscope (Nikon,
159 Tokyo, Japan) equipped with a Digital Sight DS-5Mc camera (Nikon).

160

161 **Results**

162 **Morphological features of the nasal cavity**

163 The nasal meatus of green sea turtles comprised a pair of straight tubes that
164 respectively opened as nostrils and choanae at the anterior and posterior ends, forming a
165 respiratory tract (Figure 1). The middle region of each tube contained distinct anterodorsal,
166 anteroventral and posterodorsal diverticula and a posteroventral excavation separated by
167 connective tissue containing cartilages (Figure 1C, D). The anterodorsal and anteroventral
168 diverticula appeared compressed compared with the longitudinal axis on CT images,
169 whereas the posterodorsal diverticulum assumed the form of water drops (Figure 2).

170

171 **Water inflow into the nasal cavity**

172 We simply simulated water inflow by placing the nasal cavity mold from
173 downwards (-90°) to upwards (90°) in water (Figure 3). Water filled the respiratory tract,
174 anteroventral diverticulum and anteroventral excavation, but hardly entered the
175 posterodorsal diverticulum positioned from -90° to about 40° . Water did not enter the
176 anterodorsal diverticulum when positioned horizontally (0°), but filled most of this area
177 in both the upward (about 40°) and downward (-90°) positions.

178

179 **Projection patterns of nerve bundles derived from the nasal cavity**

180 The left and right olfactory nerve tracts projected into each one of a pair of well-
181 developed olfactory bulbs that were located anterior to the cerebrum (Figure 4A). A thick
182 nerve bundle derived from the posterodorsal diverticulum formed the dorsolateral part of
183 the olfactory nerve tract (Figure 4B). The anterodorsal and anteroventral diverticula
184 projected several thin nerve bundles that formed the ventromedial part of the olfactory

185 nerve tract (Figure 4C, D). A single thin bundle derived from the posteroventral
186 excavation comprised the most medial nerve that ran across the nerves derived from the
187 anterodorsal and anteroventral diverticula, to join the anterior end of the olfactory nerve
188 tract (Figure 4C, D). Figure 4E summarizes these projections.

189

190 **Distribution pattern and histological features of three types of sensory epithelia**

191 Most of the respiratory tract from the nostrils to the choanae of the green sea turtles
192 was covered by non-sensory epithelium (Figure 5, black line), and three types of
193 sensory epithelia were separated by non-sensory epithelium in the middle of the nasal
194 cavity (Figure 5, blue, red and green lines).

195 The anterodorsal and anteroventral diverticula, as well as the medial side of the
196 respiratory tract between them, were lined with a thick epithelium (Figure 5, blue line).
197 Zones of oval and round nuclei were respectively located at the upper third and lower
198 two-thirds of the epithelium (Figure 6A). Nuclei of supporting cells arranged at the top
199 region were large and bright. Cells in the zone of round nuclei composed those resembling
200 supporting cell-like cells with large bright nuclei, and bipolar receptor cells with small
201 dark nuclei (Figure 6B). Some cells in the zone of round nuclei were positive for
202 HuC/HuD, but others were negative (Figure 6C). Basal cells were located at the bottom
203 of the epithelium, and the lamina propria did not contain gland structures (Figure 6A).

204 Sensory epithelium that occupied a relatively small area on the posteroventral
205 excavation (Figure 5, red line) also had similar histological features to the epithelium
206 covering the anterodorsal and anteroventral diverticula (Figure 7).

207 Relatively thin epithelium that exclusively lined the posterodorsal diverticulum
208 (Figure 5, green line) also contained the zones of oval and round nuclei (Figure 8A). The

209 zone of round nuclei almost completely consisted of HuC/HuD-positive bipolar receptor
210 cells (Figure 8B, C), unlike other two types of epithelia. The basal cells were located at
211 the bottom, and some well-developed olfactory glands were located in the lamina propria
212 (Figure 8A).
213

214 **Discussion**

215 The structure of the nasal cavity that functions in olfaction and respiration is diverse
216 among animal species. Comparative morphological investigations of the nasal cavity
217 helps to understand how odorants are sensed and how animals phylogenetically adapt to
218 the environment in terms of olfaction and respiration. We identified four distinct
219 structures that arise from the respiratory tract in the middle of the nasal cavity of green
220 sea turtles, and these four structures were also significant in the nose of the adult sea turtle
221 (manuscript in preparation). Among them, three have been described as diverticula
222 (Parsons 1968), but the present morphological and CT analyses uncovered a fourth
223 distinct structure, namely, a posteroventral excavation. The nasal cavity of turtles in
224 general is separated into olfactory (regio olfactoria) and intermediate (regio intermedialis)
225 regions (Parsons 1959; Bartol and Musick 2003; Schwenk 2008) that were each lined
226 with different types of epithelium. These have also been described as upper and lower
227 chambers respectively (Taniguchi and Taniguchi 2014; Nakamuta N et al. 2016;
228 Nakamuta S et al. 2016). The olfactory region refers to the sector of the nasal cavity that
229 contains mostly air to receive volatile odorants (Bartol and Musick 2003), and the
230 findings of our water inflow simulation supported the notion that the posterodorsal
231 diverticulum corresponds to the olfactory region of sea turtles (Parsons 1959; Bartol and
232 Musick 2003). The anterodorsal and anteroventral diverticula and the posteroventral
233 excavation seem to be components of the intermediate region.

234 The olfactory region of green sea turtles was covered by a relatively thin type of
235 sensory epithelium containing olfactory glands in the lamina propria. The histological
236 features of this epithelium corresponded to those of the sensory epithelium in the olfactory
237 region of other turtles (Graziadei and Tucker 1969; Nakamuta N et al. 2016; Nakamuta S

238 et al. 2016) including loggerhead sea turtles (Saito et al. 2000), and it is similar to the
239 olfactory epithelium of mammals. Therefore, our findings suggested that the olfactory
240 region of sea turtles plays a role in the reception of volatile odorants.

241 The intermediate region where water enters, contained two thick types of sensory
242 epithelia without olfactory glands, indicating that these epithelia receive water-soluble
243 odorants. Among structures in this region, the posteroventral excavation was lined by a
244 type of sensory epithelium that differed from that covering the anterodorsal and
245 anteroventral diverticula, and a nerve bundle derived from this excavation extended solely
246 to the olfactory nerve tract. These findings suggested that the excavation and the other
247 intermediate region receive different odorants and transfer the information through a
248 different circuit.

249 The zone of round nuclei in sensory epithelia in the intermediate region contained
250 HuC/HuD-negative cells. Because HuC/HuD proteins are mainly expressed in developing
251 neurons, it is possible that receptor cells that differentiated a long time ago did not react
252 with anti-HuC/HuD antibody. In addition, supporting-like cells were histologically found
253 in the zone of round nuclei, suggesting that these cells reflected to a high number of
254 HuC/HuD-negative cells. Because this zone in the intermediate region of terrestrial and
255 freshwater turtles contains few non-receptor cells (Graziadei and Tucker 1969; Nakamuta
256 N et al. 2016; Nakamuta S et al. 2016), the supporting-like cells seem unique in sensory
257 epithelia in the intermediate region of sea turtles.

258 Olfactory stimuli via air and water flow are recognized by odorant receptors
259 expressed in receptor cells, and odorant receptors in vertebrates are mainly classified as
260 olfactory (OR), vomeronasal types 1 (V1R) and 2 (V2R), and trace amine-associated
261 (TAAR) receptors. Wang et al. (2013) revealed the draft genome of green sea turtle and

262 showed that it contains intact 159 Class I OR that generally seem hydrophilic, and intact
263 95 Class II OR that seem hydrophobic. Genbank refseq database shows that the genome
264 of green sea turtles also encodes twelve intact TAAR (Supplementary Table 1). On the
265 other hand, only two intact V1R and a single V2R are encoded in green sea turtle genome
266 (Supplementary Table 1), indicating that both V1R and V2R families have degenerated
267 in sea turtles. Therefore, the sensory epithelia in the intermediate region in the nasal cavity
268 of sea turtles might receive water-soluble odorants mainly via Class I OR and/or TAAR
269 families, although further evaluation *in situ* and embryological studies are required to
270 understand the features of the sensory epithelia in the nasal cavity of sea turtles.

271 The present study revealed structural details of the nasal cavity and three
272 independent sensory epithelia that project nerve bundles to the olfactory bulbs of juvenile
273 green sea turtles. These findings provide a basic understanding of olfactory sensing in
274 juveniles, and further studies will focus on adult sea turtles.

275

276 **Conflict of interests**

277 The authors have no conflicts of interest to declare.

278

279 **Funding**

280 This study was supported by the Okinawa Churashima Foundation [No. 205 to
281 C.K.].

282

283 **Acknowledgments**

284 We thank the staff of the Everlasting Nature of Asia (ELNA) for cooperation with
285 this study, and Mr. Hidenori Otsubo and the staff of the Information Processing Center,
286 Obihiro University of Agriculture and Veterinary Science for advice regarding three-
287 dimensional printing.

288

289 **References**

- 290 Bartol SM, Musick JA. 2003. Sensory biology of sea turtles. In: Lutz PL, Musick JA,
291 Wyneken J (eds) *The Biology of Sea Turtles*, vol II. CRC Press, Boca Raton. pp. 79–
292 102.
- 293 Bowen BW, Karl SA. 2007. Population genetics and phylogeography of sea turtles. *Mol*
294 *Ecol.* 16:4886–4907.
- 295 Endres CS, Putman NF, Lohmann KJ. 2009. Perception of airborne odors by loggerhead
296 sea turtles. *J Exp Biol.* 212:3823–3827.
- 297 Endres CS, Lohmann KJ. 2013. Detection of coastal mud odors by loggerhead sea turtles:
298 a possible mechanism for sensing nearby land. *Mar Biol.* 160:2951–2956.
- 299 Frazer NB, Ehrhart LM. 1985. Preliminary growth models for green, *Chelonia mydas*,
300 and loggerhead, *Caretta caretta*, turtles in the wild. *Copeia.* 1985:73–79.
- 301 Graziadei PPC, Tucker D. 1970. Vomeronasal receptors in turtles. *Z Zellforsch.* 105:498–
302 514.
- 303 Gunasegaran JP. 2010. *Textbook of Histology and a Practical Guide*, 2nd ed. New Delhi,
304 Elsevier.
- 305 Hirayama R. 1998. Oldest known sea turtle. *Nature.* 392:705–708.
- 306 Kondoh D, Nashimoto M, Kanayama S, Nakamuta N, Taniguchi K. 2011. Ultrastructural
307 and histochemical properties of the olfactory system in the Japanese jungle crow,
308 *Corvus macrorhynchos*. *J Vet Med Sci.* 73:1007–1014.
- 309 Kondoh D, Yamamoto Y, Nakamuta N, Taniguchi K, Taniguchi K. 2010. Lectin
310 histochemical studies on the olfactory epithelium and vomeronasal organ in the
311 Japanese striped snake, *Elaphe quadrivirgata*. *J Morphol.* 271:1197–1203.
- 312 Li C, Wu XC, Rieppel O, Wang LT, Zhao LJ. 2008. An ancestral turtle from the Late

313 Triassic of southwestern China. *Nature*. 456:497–501.

314 Limpus C, Kamrowski RL. 2013. Ocean-finding in marine turtles: the importance of low
315 horizon elevation as an orientation cue. *Behaviour*. 150:863–893.

316 Manton M, Karr A, Ehrenfeld DW. 1972. Chemoreception in the migratory sea turtle,
317 *Cheronia mydas*. *Biol Bull*. 143:184–195.

318 Nakamuta N, Nakamuta S, Kato H, Yamamoto Y. 2016. Morphological study on the
319 olfactory systems of the snapping turtle, *Chelydra serpentina*. *Tissue Cell*. 48:145–
320 151.

321 Nakamuta S, Yokosuka M, Taniguchi K, Yamamoto Y, Nakamuta N. 2016.
322 Immunohistochemical analysis for G protein in the olfactory organs of soft-shelled
323 turtle, *Pelodiscus sinensis*. *J Vet Med Sci*. 78:245–250.

324 Nakamuta S, Kusuda S, Yokosuka M, Taniguchi K, Yamamoto Y, Nakamuta N. 2018.
325 Immunohistochemical analysis of the development of olfactory organs in two species
326 of turtles *Pelodiscus sinensis* and *Mauremys reevesii*. *Acta Histochem*. 120: 806–813.

327 Parsons TS. 1959. Nasal anatomy and the phylogeny of reptiles. *Evolution*. 13:175–187.

328 Parsons TS. 1968. Evolution of the nasal structure in the lower tetrapods. *Am Zoologist*.
329 7:397–413.

330 Romer AS, Parsons TS. 1977. *The Vertebrate Body*, 5th ed. Philadelphia, Saunders.

331 Saito K, Shoji T, Uchida I, Ueda H. 2000. Structure of the olfactory and vomeronasal
332 epithelia in the loggerhead turtle *Caretta caretta*. *Fish Sci*. 66:409–411.

333 Schwenk K. 2008. Comparative anatomy and physiology of chemical senses in nonavian
334 aquatic reptiles. In: Thewissen JGM, Nummels S. (eds) *Sensory Evolution on the*
335 *Threshold. Adaptations in Secondarily Aquatic Vertebrates*. Berkeley, Univ. of
336 California Press. pp. 65–81.

337 Shi P, Zhang J. 2007. Comparative genomic analysis identifies an evolutionary shift of
338 vomeronasal receptor gene repertoires in the vertebrate transition from water to land.
339 *Genome Res.* 17:166–174.

340 Taniguchi K, Taniguchi K. 2014. Phylogenic studies on the olfactory system in
341 vertebrates. *J Vet Med Sci.* 76:781–788.

342 Wang Z, Pascual-Anaya J, Zadissa A, Li W, Niimura Y, Huang Z, Li C, White S, Xiong
343 Z, Fang D, *et al.* 2013. The draft genomes of soft-shell turtle and green sea turtle yield
344 insights into the development and evolution of the turtle-specific body plan. *Nat Genet.*
345 45:701–706.

346

347 **Figure Legends**

348 **Figure 1.** Morphological features of nasal cavity of green sea turtles.

349 (A) Left lateral view of the head. Boxed area indicates the nasal area and corresponds to
350 panels (B-D). (B) Outer nasal cartilages after removing bones encircling nasal area. (C)
351 Internal structure of nasal cavity after removing left half. (D) Alcian blue (pH 2.5) and
352 alizarin red stained image corresponding to panel (C). Connective tissue containing
353 cartilages (arrowheads) positive for Alcian blue distinctly separates anterodorsal (1) and
354 anteroventral (2) diverticula, posteroventral excavation (3) and posterodorsal
355 diverticulum (4). *Nostrils.

356

357 **Figure 2.** Internal structures of nasal cavity of green sea turtles.

358 (A) Three-dimensional image of head reconstructed from computed tomographic (CT)
359 images. Air in nasal cavity is extracted in yellow to visualize internal structure of nasal
360 cavity. Boxed area corresponds to panels (B-E). (B) CT image of nasal cavity shows four
361 distinct structures. (C-E) Left lateral (C), frontal (D) and dorsal (E) views of three-
362 dimension reconstructed images of the nasal cavity. Anterodorsal (1) and anteroventral
363 (2) diverticula, posteroventral excavation (3) and posterodorsal diverticulum (4).
364 *Nostrils.

365

366 **Figure 3.** Simulation of water inflow into nasal cavity.

367 Model of internal structure of nasal cavity (upper). Silicon molding submerged in water
368 at horizontally (0°), upwards (about 40°) and downwards (90°) (middle), and schemes of
369 water inflow at each location (lower). Upper side is water surface. Minimal amount of
370 water enters posterodorsal diverticulum (arrows). Water fills anterodorsal diverticulum

371 (arrowheads) in upward and downward positions. Blue and white areas in nasal cavity
372 indicate water and air, respectively. *Nostrils.

373

374 **Figure 4.** Projection of nerve bundles derived from nasal cavity.

375 (A) Dorsal view of nasal cavity and anterior brain region after removing skull. Left side
376 is anterior. Left and right olfactory nerve tracts (arrow) originate from nasal cavity (NC)
377 and reach olfactory bulbs (OB) located at front of cortex (Cor). *Orbit. (B) Dorsal view
378 of right olfactory nerve tract. Left olfactory nerve tract is removed. Dorsolateral part (dl)
379 is derived from posterodorsal diverticulum (4), and ventromedial part (vm) is derived
380 from other regions of nasal cavity. (C and D) Left lateral view (upper) and trace (lower)
381 of nerve distribution in right nasal cavity before (C) and after (D) removing nasal septum.
382 Several thin nerve bundles derived from anterodorsal (1) and anteroventral (2) diverticula
383 form ventromedial part (vm) of olfactory nerve tract (blue lines). Single thin bundle of
384 nerves (arrows) is derived from posteroventral excavation (3) and runs in most medial
385 region (red lines). Dorsolateral part (dl) of olfactory nerve tract is derived from
386 posterodorsal diverticulum (green lines). (E) Scheme of left lateral view of nerve
387 distribution in right nasal cavity according to panels (C and D).

388

389 **Figure 5.** Distribution of epithelia in nasal cavity.

390 Lateral view of nasal cavity region (top) and frontal section of nasal cavity based on
391 histological findings (bottom). Straight lines with alphabetical letters in top panel indicate
392 positions corresponding to images with same letters. Blue, red and green lines indicate
393 separate types of sensory epithelia. Black line indicates non-sensory epithelium.
394 Anterodorsal (1) and anteroventral (2) diverticula, posteroventral excavation (3) and

395 posterodorsal diverticulum (4).

396

397 **Figure 6.** Histological features of sensory epithelium covering anterodorsal and
398 anteroventral diverticula.

399 (A) Whole epithelium stained with hematoxylin-eosin. Arrowheads indicate basal cells.

400 ZON, zone of oval nuclei; ZRN, zone of round nuclei. (B) High magnification of ZRN.

401 Arrows and arrowheads indicate nuclei of supporting-like cells and bipolar receptor cells,

402 respectively. (C) Anti-HuC/HuD immunoreaction in ZRN. Arrows and arrowheads

403 indicate negative and positive cells, respectively. Bar = 30 μ m.

404

405 **Figure 7.** Histological features of sensory epithelium covering posteroventral excavation.

406 (A) Whole epithelium stained with hematoxylin-eosin. Arrowheads indicate basal cells.

407 ZON, zone of oval nuclei; ZRN, zone of round nuclei. (B) High magnification of ZRN.

408 Arrows and arrowheads indicate nuclei of supporting-like cells and bipolar receptor cells,

409 respectively. (C) Anti-HuC/HuD immunoreaction in ZRN. Arrows and arrowheads

410 indicate negative and positive cells, respectively. Bar = 30 μ m.

411

412 **Figure 8.** Histological features of sensory epithelium covering posterodorsal
413 diverticulum.

414 (A) Whole epithelium with olfactory gland (asterisk) in lamina propria, stained with

415 hematoxylin-eosin. Arrowheads indicate basal cells. ZON, zone of oval nuclei; ZRN,

416 zone of round nuclei. (B) High magnification of ZRN. Arrows indicate nuclei of bipolar

417 receptor cells. (C) Anti-HuC/HuD immunoreaction in ZRN. Arrowheads indicate positive

418 cells. Bar = 30 μ m.

Supplementary Table 1.

TAAR, V1R and V2R genes in green sea turtle based on the genomic information.

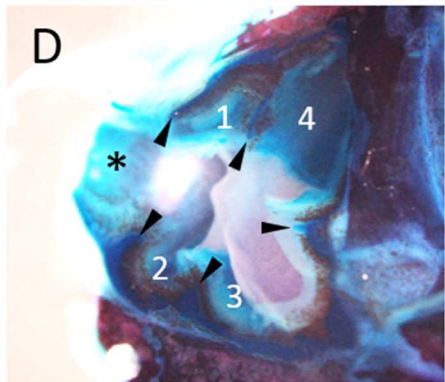
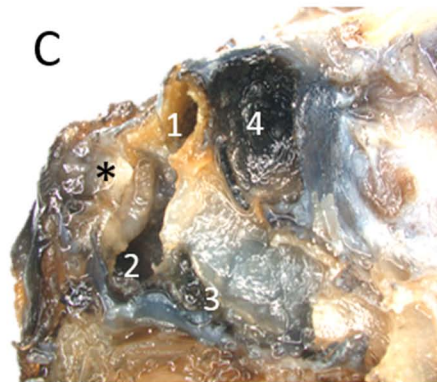
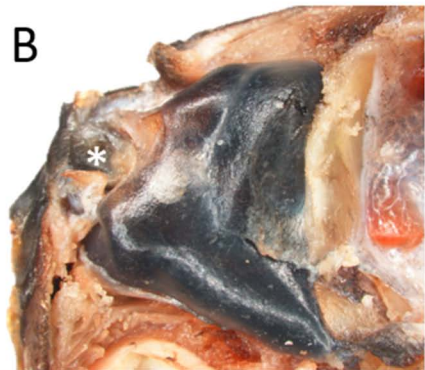
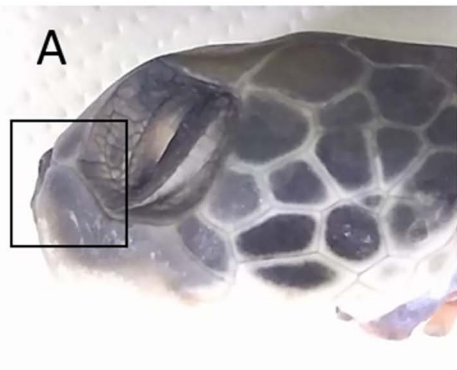
Receptor family	Genbank accession
TAAR*	XM_007062262.2
	XM_007062261.1
	XM_007062260.2
	XM_007062259.2
	XM_007062257.1
	XM_007062256.1
	XM_007062255.1
	XM_007062254.1
	XM_007062253.2
	XM_007062247.2
	XM_007062246.2
	XM_027824652.1
	XR_443470.2
V1R [†]	XM_007059608.1
	XM_007067150.1
V2R [†]	(EMP28964.1; protein database) [‡]

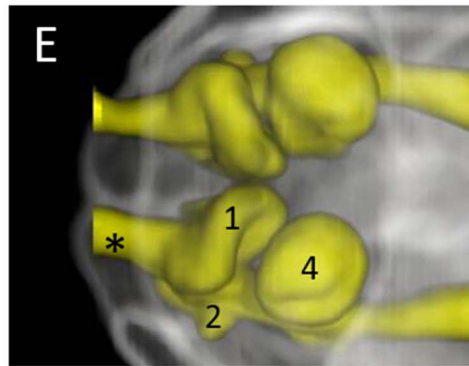
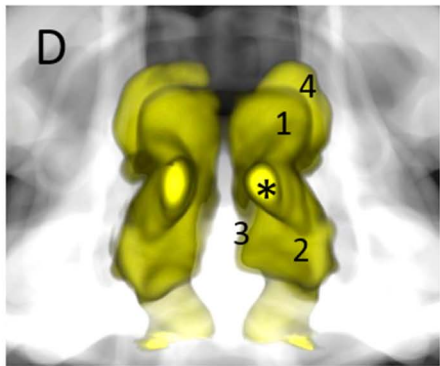
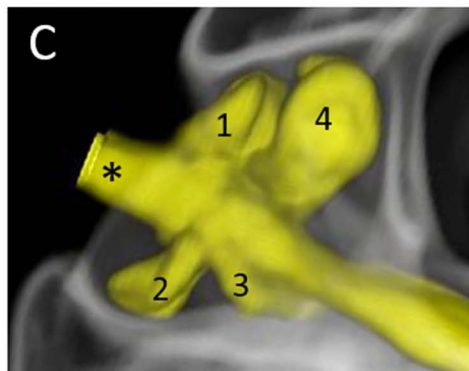
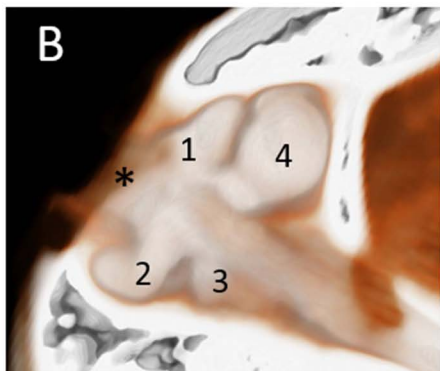
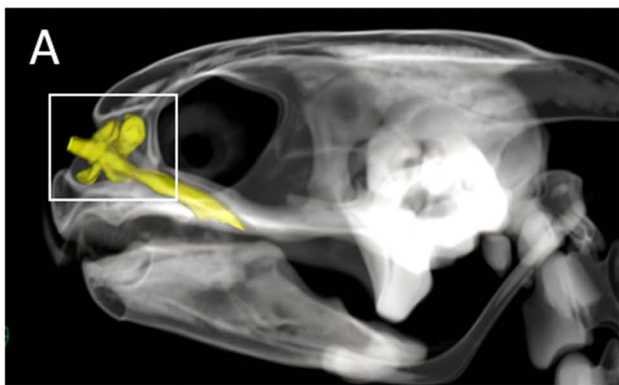
* The locus of TAAR on chromosome are conserved among reptiles, and TAAR genes are located near vanin 1 gene to form a gene cluster. We counted the number of TAAR genes on contig: NW_006637070.1.

[†] TBLASTN search (Camacho et al. 2009) were performed on refseq RNA sequences to retrieve green sea turtle V1R and V2R genes. Query sequences were total 244 and 215 protein sequences of V1R and V2R, respectively, in four vertebrates; zebrafish (*Danio rerio*), western clawed frog (*Xenopus tropicalis*), mouse (*Mus musculus*) and Chinese soft-shell turtle (*Pelodiscus sinensis*).

[‡] Blast results did not show any V2R in green sea turtle, but protein database suggests one V2R and genome information indicates one pseudo gene (Gene ID: 102943443) in green sea turtles.

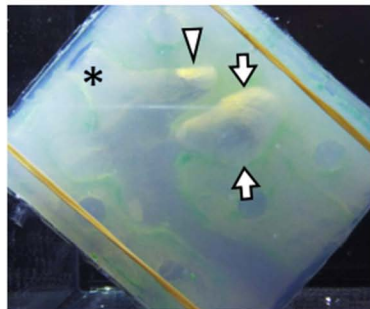
Camacho C, Coulouris G, Avagyan V, Ma N, Papadopoulos J, Bealer K, Madden TL. 2009. BLAST plus: architecture and applications. *BMC Bioinformatics*. 10:1.



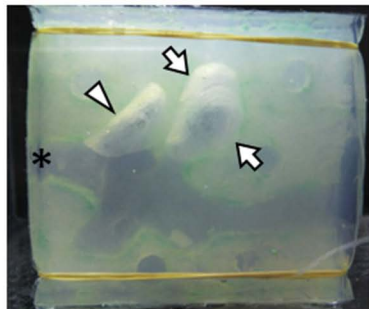




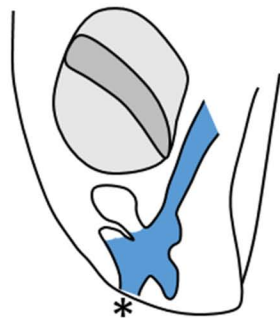
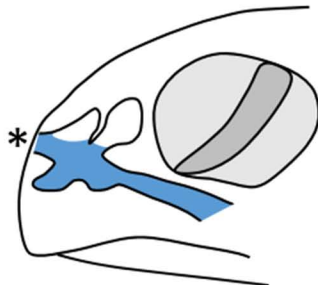
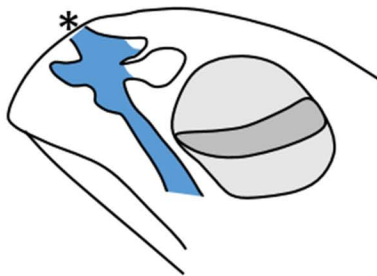
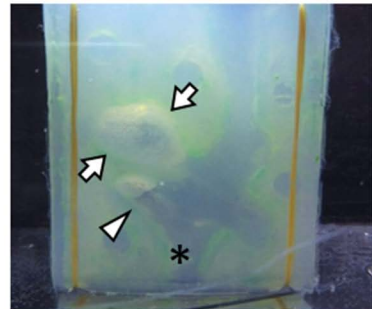
Upward (about 40°)

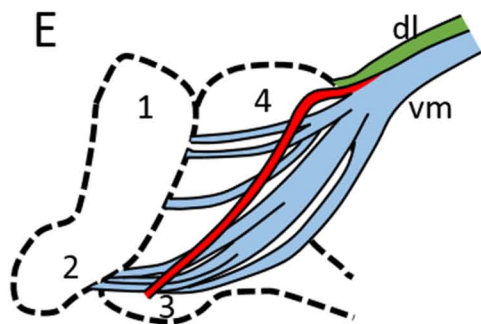
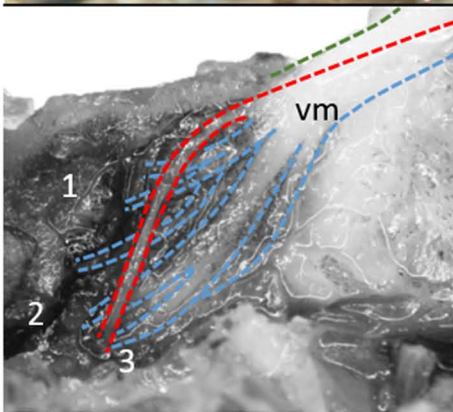
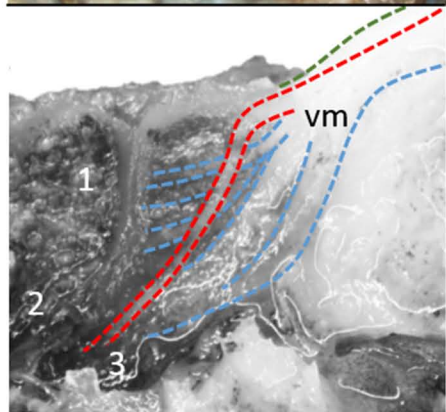
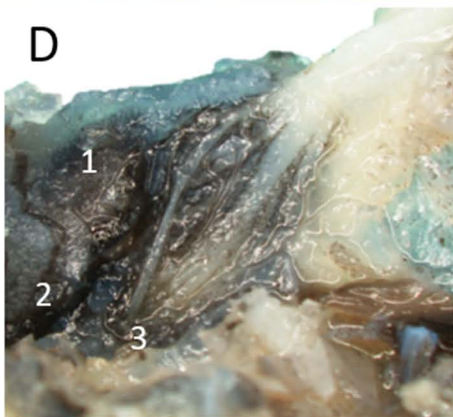
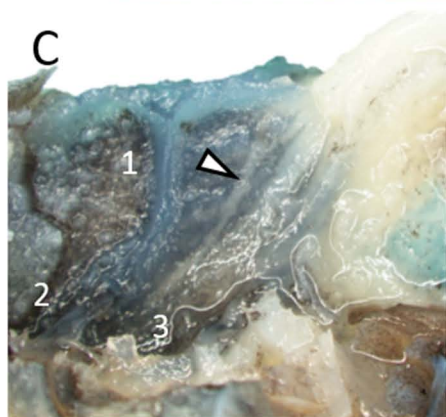
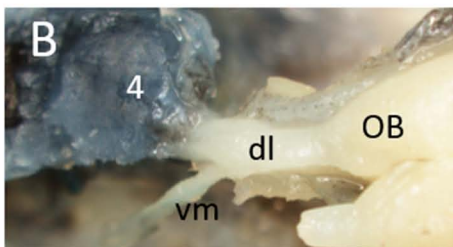
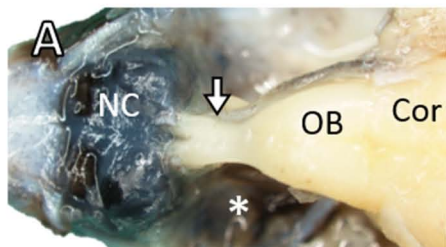


Horizontal (0°)

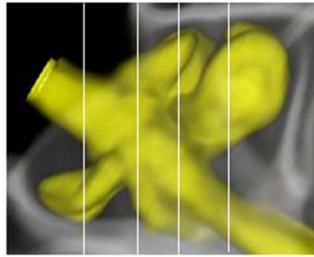


Downward (-90°)

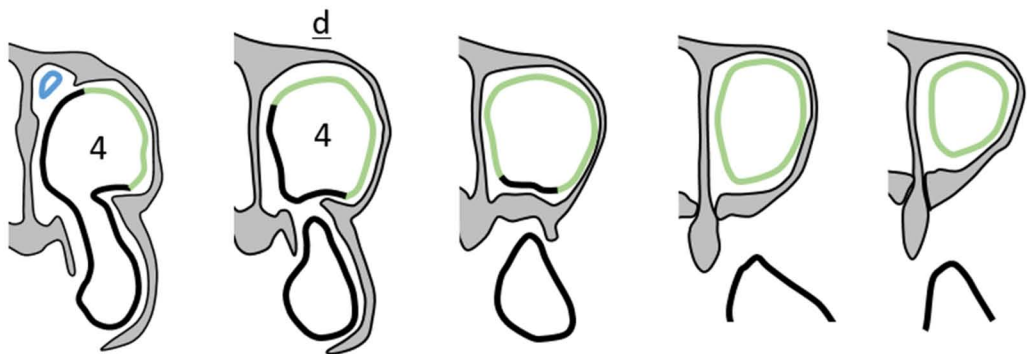
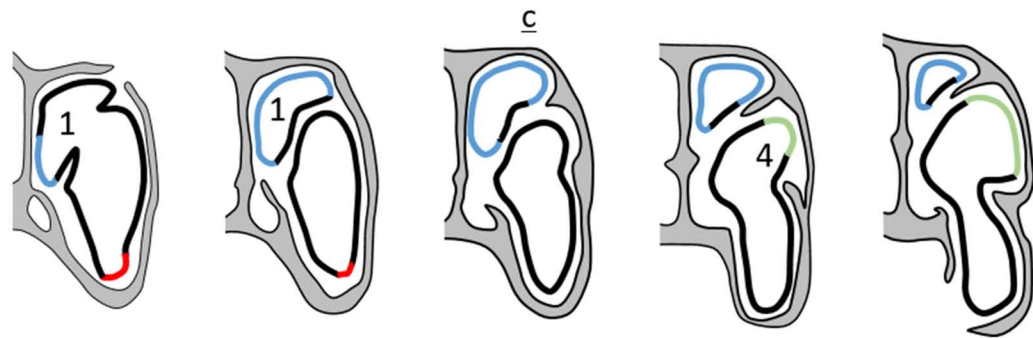
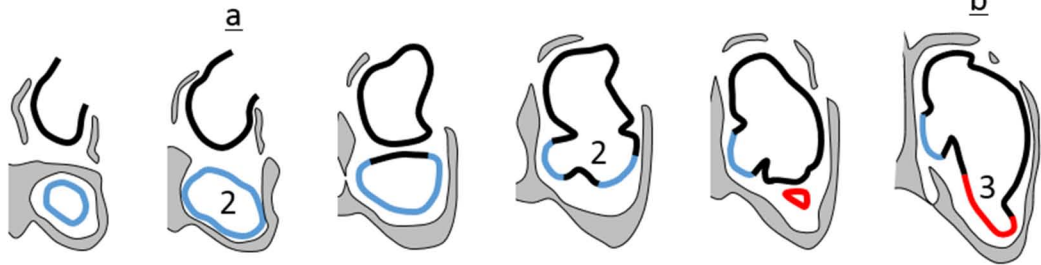




a b c d



anterior



posterior



